Electronic Supplementary Material (ESI) for Chemical Science.
This journal is © The Royal Society of Chemistry 2017

Fluorinated Eu^{II}-based multimodal contrast agent for temperature- and redox-responsive magnetic resonance imaging

Lina A. Basal,[a] Matthew D. Bailey,[a] Jonathan Romero,[b] Meser M. Ali,[c] Lyazat Kurenbekova,[d] Jason Yustein,[d,e] Robia G. Pautler,[b,]* and Matthew J. Allen[a,]*

[a] Department of Chemistry, Wayne State University, 5101 Cass Avenue, Detroit, Michigan 48202, United States [b] Department of Molecular Physiology and Biophysics, Baylor College of Medicine, One Baylor Plaza, Houston, Texas 77030, United States [c] Department of Neurosurgery, Henry Ford Hospital, 1 Ford Place, Detroit, Michigan 48202, United States [d] Integrative Molecular and Biomedical Sciences, Baylor College of Medicine, Houston, TX 77030, USA [e] Department of Pediatrics, Texas Children's Cancer and Hematology Centers, Baylor College of Medicine, Houston, TX 77030, USA

*E-mail: rpautler@bcm.edu
mallen@chem.wayne.edu

Experimental Procedures

Commercially available chemicals were of reagent-grade purity or better and were used without further purification unless otherwise noted. DOWEX-Na^+ was prepared as previously reported.[1] Water was purified using a PURELAB Ultra Mk2 water purification system (ELGA). Samples of **$2Eu^{II}$** and **$3Eu^{II}$** were prepared in a wet (water but no O_2) glovebox under an atmosphere of N_2.

^{1}H and ^{13}C-NMR spectra were acquired using an Agilent MR-400 (399.78 MHz for ^{1}H and 100.53 MHz for ^{13}C), a Varian MR-400 (399.69 MHz for ^{1}H and 100.51 MHz for ^{13}C), or a Varian VNMRS-500 (499.42 MHz for ^{1}H and 125.59 MHz for ^{13}C) spectrometer. ^{19}F-NMR spectra were obtained using a Mercury 400 (376 MHz for ^{19}F) spectrometer or a Bruker BioSpec 9.4 T horizontal bore MRI scanner. Chemical shifts are reported relative to residual solvent signals or internal standard (CH_3OD: ^{1}H δ 3.31; $CDCl_3$: ^{1}H δ 7.27, ^{13}C δ 77.23, ^{19}F δ 0.00 ($CFCl_3$ internal standard in $CDCl_3$); DMSO-d_6: ^{1}H δ 2.50, ^{13}C δ 39.52; DMF-d_7: ^{13}C δ 29.76; ^{19}F δ 0.00 ($CFCl_3$ internal standard in DMF-d_7); D_2O: ^{1}H δ 7.27, ^{19}F: δ –78.20 (NaOTf internal standard in D_2O). NMR data are assumed to be first order and the multiplicity is reported as “s” = singlet, “d” = doublet, “dd” = doublet of doublets, “q” = quartet, and “brs” = broad singlet. Italicized elements are those that are responsible for the shifts. Correlation spectroscopy (COSY), distortionless enhancement by polarization transfer (DEPT), and heteronuclear multiple quantum coherence (HMQC) spectra were used to assign spectral peaks.

CEST NMR spectra were acquired on a Varian VNMRS-500 (499.42 MHz) spectrometer. The sample temperature was 22.5 °C, and a saturation frequency array was used with a saturation time of 4 s, a saturation power of 24 μT, a 45° observation pulse, an initial frequency of 75 ppm (37,500 Hz), a final frequency of –75 ppm (–37,500 Hz), and increments of 2 ppm (1000 Hz). All samples were in aqueous 3-morpholinopropane-1-sulfonic acid buffer (pH 7.0), 10% D_2O, with a concentration of Eu of 8 mM.

Elemental analyses (C, H, and N) were performed by Midwest Microlab (Indianapolis). Thermal gravimetric analysis was performed on an SDT-2960. Thermal gravimetric analysis (TGA) was recorded at 10 °C/min under flowing nitrogen using an SDT-2960 TGA/DTA. Concentrations of Eu were determined using energy-dispersive X-ray fluorescence (EDXF) spectroscopy at the Lumigen Instrument Center in the Department of Chemistry at Wayne State University. All dilutions were performed with 2% HNO_3, which was also used for blank samples during calibration. Calibration curves were created using the ^{153}Eu isotope ion count for 1–200 ppb concentration range (diluted from Fluka ICP standard solution). High-resolution electrospray ionization mass spectrometry (HRMS) were recorded using a Waters LCT Premier Xe time-of-flight high-resolution mass spectrometer.

Coupled liquid chromatography and mass spectrometry (LCMS) was performed on a Shimadzu LCMS 2010EV. Sample of either **$2Eu^{III}$** or mouse urine collected post-imaging were injected onto an analytical VivaC18 RESTEK column equipped with a VivaC8 guard column. Elution was at a flow rate of 1 mL/min using an isocratic eluent of 95% acetonitrile in water. The mass associated with the complex in both cases was observed at 2.8 minutes.

Cyclic voltammetry was performed using a glassy carbon working electrode, platinum wire auxiliary electrode and Ag/AgCl reference electrode coupled with a Pine Wavenow USB. Acquisition parameters were eight segments, initial potential of 0 V, final potential of –1.5 V, and a sweep rate of 100 mV/s in dimethylformamide.

UV–visible absorbance spectra were measured using a Shimadzu UVmini-1240 spectrophotometer, and samples were loaded in quartz cuvettes under an atmosphere of N_2. Emission and excitation spectra were recorded using a HORIBA Jobin Yvon Fluoromax-4 spectrofluorometer.

T_1 values were measured with inversion-recovery experiments using a Varian VNMRS-500 (11.7 T) from 16.5 to 40.5 °C. Relaxivity was obtained from the slope of $1/T_1$ (s^{-1}) versus concentration of either **$2Eu^{II}$** or **$3Eu^{II}$** ([3-(*N*-morpholino)propanesulfonic acid], pH 7.0) using a linear regression. Measurements were performed in triplicate with independently prepared solutions, and the relaxivity values are reported as the mean ± standard error of the mean of the independent measurements.

All animal studies were done in accordance with protocols preapproved by the Institutional Animal Care and Use Committee of Baylor College of Medicine. T_1-weighted and ^{19}F MRI scans were performed with a Bruker BioSpec 9.4T horizontal bore MRI scanner equipped with 20 cm bore. Images were acquired with a body coil while using a heater set to

37 °C. A ketamine/xylazine cocktail was used for anesthesia to avoid crossover signals in the images from the fluorine typically observed with isoflurane. The phantom images for T_1-weighted images were acquired using an echo time of 8.5 ms, repetition time of 1500 ms, flip angle of 180 degrees, 9 image slices at 1 mm thickness, a field-of-view of 5 cm × 5 cm, and matrix size of 256 mm × 256 mm. Mouse images for T_1-weighted images were acquired using a three-dimensional fast low angle shot magnetic resonance imaging (FLASH) sequence with an echo time of 1.931 ms, a repetition time of 6.0 ms, a field-of-view of 40 mm × 35 mm × 25 mm, and a matrix size of 128 mm × 128 mm × 16 mm. For the first scan, the number of repetitions was 40. For subsequent scans, the number of repetitions was 1. **2Eu$^{\mathbf{II}}$** was injected into the intraperitoneal cavity 2 minutes into the first scan. A single pulse ^{19}F spectra with a repetition time of 2000 ms and 60 averages was acquired to monitor the appearance of the ^{19}F spectra. Fluorine-19 phantom images were acquired using an echo time of 8.952 ms, a repetition time of 2000 ms, a flip angle of 180 degrees, two image slices of 8 mm thickness, a field-of-view of 4 cm × 4 cm, and an in-plane resolution of 256 μm × 256 μm. A total of five mice were imaged, and representative images are in the manuscript.

CEST images were acquired on a Bruker Small Animal scanner 7.0 T (299.44 MHz) horizontal bore MRI scanner. Images were acquired using an echo time of 12.7 ms, a repetition time of 5000 ms, a field-of-view of 24 mm × 24 mm, a power of 16 μT, a matrix size of 256 × 192, a rare factor of 8, and 3 averages.

Synthetic Procedures and Characterization

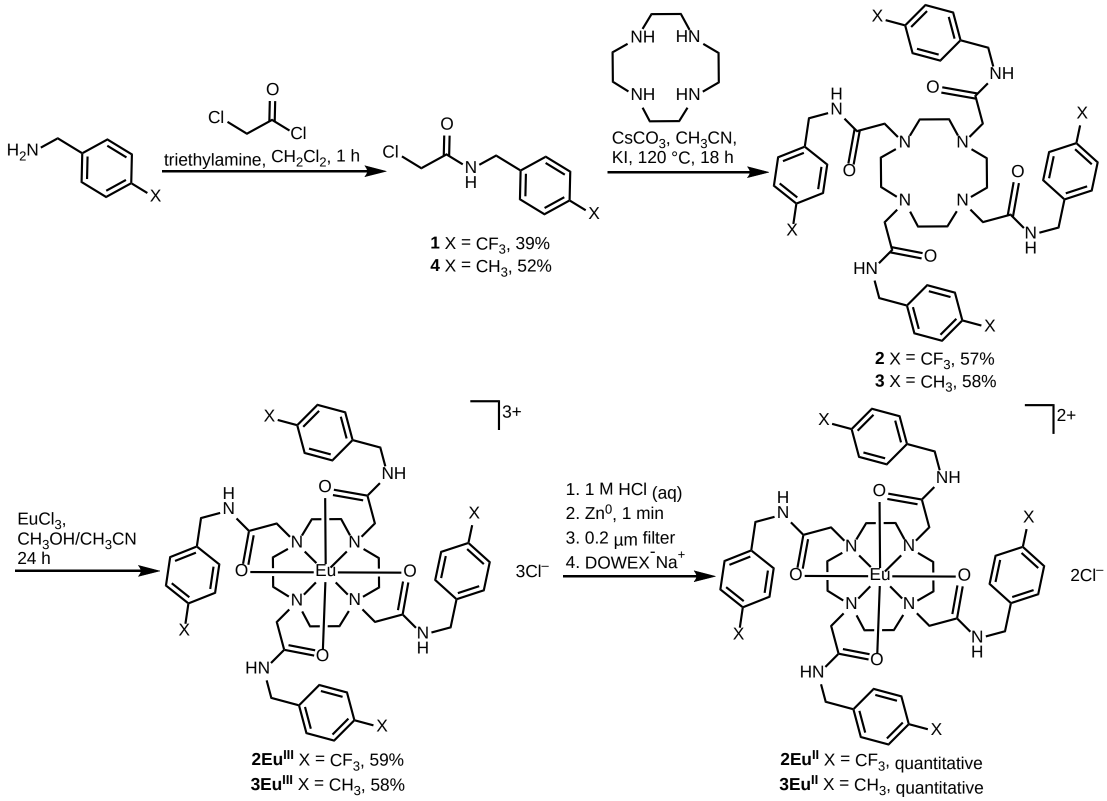

Figure S1. Reaction scheme for complexes studied

2-Chloro-*N*-(4-(trifluoromethyl)benzyl)acetamide (1): To a stirring solution of (4-(trifluoromethyl)phenyl)methanamine (5.2563 g, 30.010 mmol) and triethylamine (4.25 mL, 30.5 mmol) in CH_2Cl_2 (5 mL) at 0 °C, a solution of chloroacetyl chloride (2.60 mL, 32.5 mmol) in CH_2Cl_2 (17 mL) was added dropwise. The resulting reaction mixture was stirred for 30 minutes at 0 °C followed by 30 minutes at ambient temperature. The mixture was filtered through a fine glass frit, and the solid was washed with CH_2Cl_2 (5 × 5 mL). The organic layer was washed with HCl (2 M, aqueous, 2 × 10 mL) followed by brine (3 × 10 mL), and the organic layer was dried over sodium sulfate. Solvent was removed under reduced pressure to yield a tan solid that was crystallized from CH_2Cl_2 to yield a white solid (3.0081 g, 39%). ^{1}H NMR (400 MHz, $CDCl_3$): δ 4.11 (s, 2H, ClC*H*$_2$), 4.55 (d, *J* = 6.4 Hz, 2H, NC*H*$_2$), 7.05 (brs, 1H, N*H*), 7.51 (dd, *J* = 79.7, 7.8 Hz, 4H, C*H*); ^{13}C NMR (125 MHz, $CDCl_3$): δ 42.7 (Cl*C*H$_2$), 43.4 (N*C*H$_2$), 124.2 (q, ^1J = 272.1 Hz, *C*F$_3$), 125.8 (q, ^3J = 3.8 Hz, CF$_3$C*C*H), 128.0 (*C*H), 130.1 (q, ^2J = 32.6 Hz, CF$_3$*C*), 141.7, 166.4. ^{19}F NMR (376 MHz, $CDCl_3$): δ –63.1 (s, C*F*$_3$); HRMS (*m*/*z*): [M + H]$^+$ calcd. for $C_{10}H_{10}ClF_3NO$, 252.0403; found, 252.0401.

^{1}H

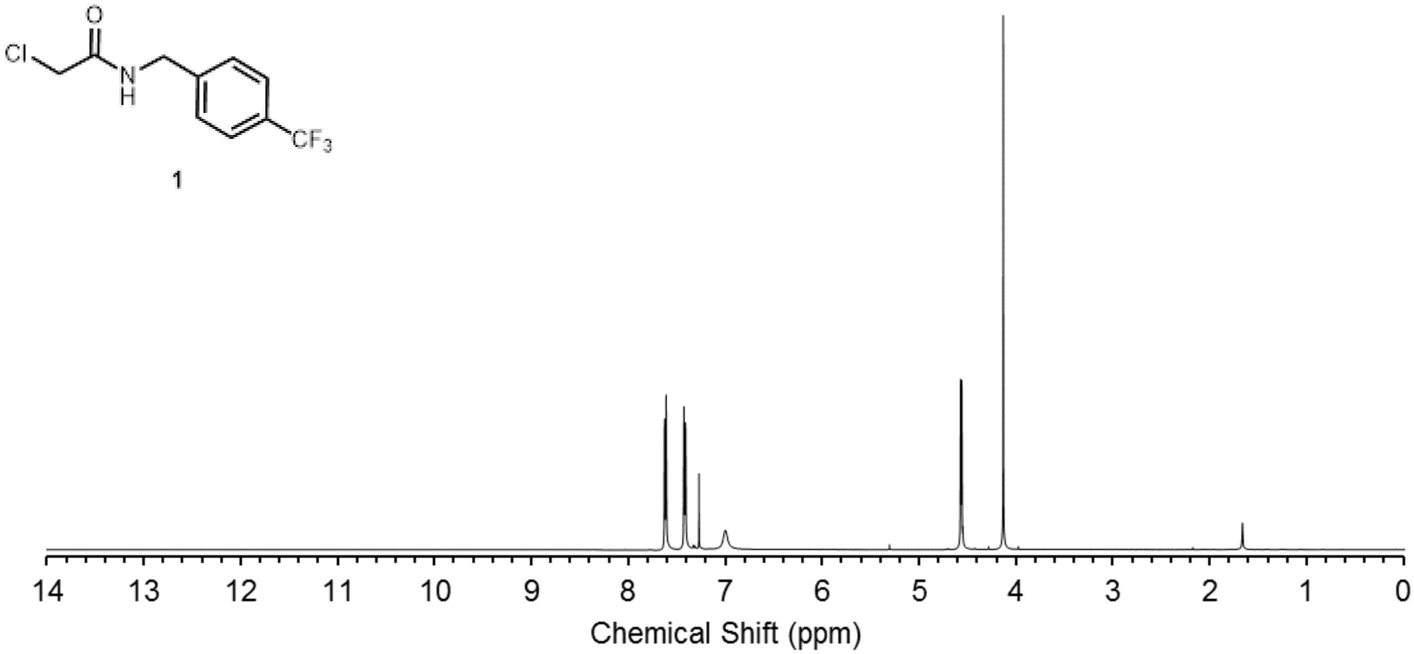
Cl
O
N
H
CF$_3$
1
14
13
12
11
10
9
8
7
6
5
4
3
2
1
0
Chemical Shift (ppm)

^{13}C

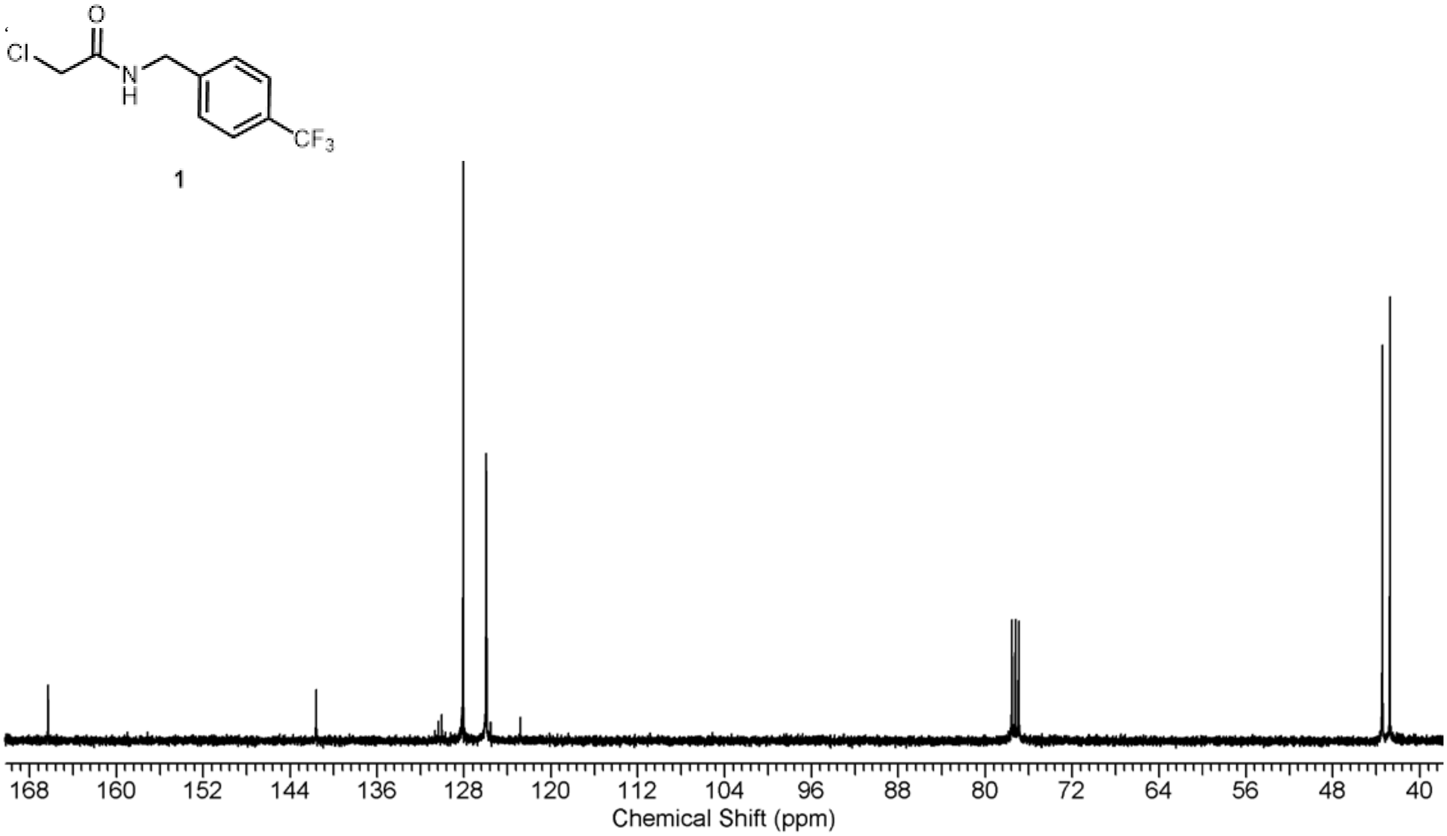
Cl
O
N
H
CF$_3$
1
168
160
152
144
136
128
120
112
104
96
88
80
72
64
56
48
40
Chemical Shift (ppm)

^{19}F

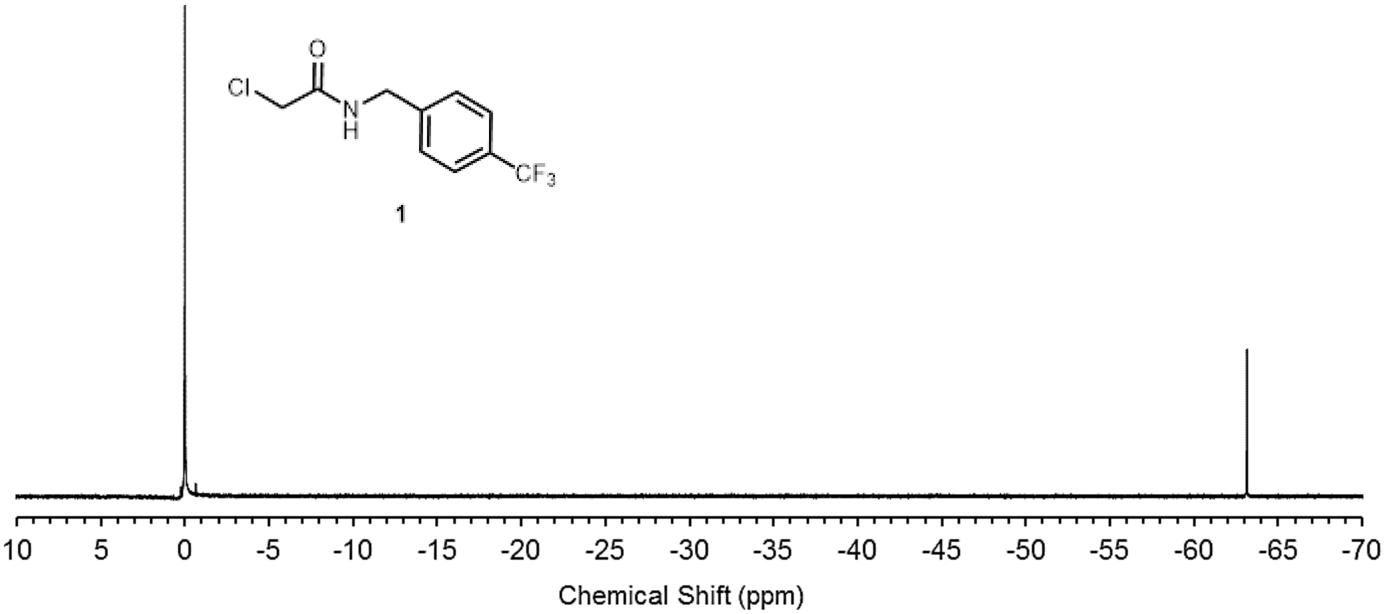

2,2',2'',2'''-(1,4,7,10-Tetraazacyclododecane-1,4,7,10-tetrayl)tetrakis(*N*-(4-(trifluoromethyl)benzyl)acetamide) (2): A stirring mixture of **1** (1.7071 g, 6.7842 mmol), Cs_2CO_3 (3.5283 g, 10.829 mmol), cyclen (0.2520 g, 1.463 mmol), potassium iodide (0.010 mg, 0.060 mmol), and acetonitrile (60 mL) was heated to 120 °C. After 18 h, the mixture was filtered while hot through a fine glass frit, and the filtrate was concentrated under reduced pressure to yield a pale yellow solid that was crystallized from acetonitrile to yield a white solid (854 mg, 57%). ^{1}H NMR (500 MHz, DMSO-d_6): δ 2.60 (s, 16H, C*H*$_2$C*H*$_2$), 3.03 (s, 8H, NC*H*$_2$CO), 4.32 (d, *J* = 5.5 Hz, 8H, OCNHC*H*$_2$), 7.50 (dd, *J* = 96.5, 7.7 Hz, 16H, C*H*), 8.45 (s, 4H, OCN*H*CH$_2$); ^{13}C NMR (125 MHz, DMF-d_7): δ 42.2 (OCNH*C*H$_2$), 54.3 (*C*H$_2$*C*H$_2$), 58.8 (OC*C*H$_2$), 125.0 (q, ^{1}*J* = 271.7 Hz, *C*F$_3$), 125.5 (q, ^{3}*J*= 4.0 Hz, CF$_3$C*C*H), 128.3 (CH$_2$C*C*H), 128.3 (q, ^{2}*J* = 31.6 Hz, CF$_3$*C*), 145.3, 171.3; ^{19}F NMR (376 MHz, DMF-d_7): δ –61.1 (s, C*F*$_3$); HRMS (*m*/*z*): $[M + H]^+$ calcd. for $C_{48}H_{53}F_{12}N_8O_4$, 1033.3998; found, 1033.4021.

^{1}H

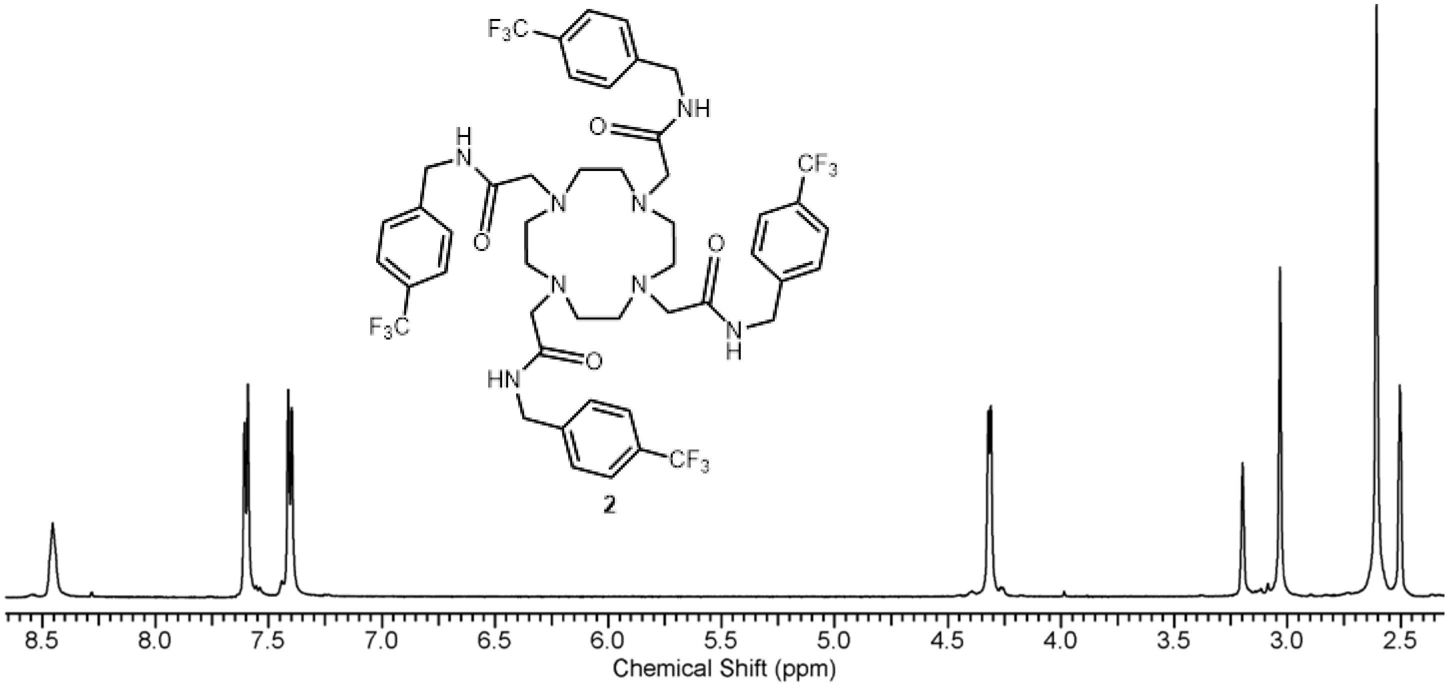

^{13}C

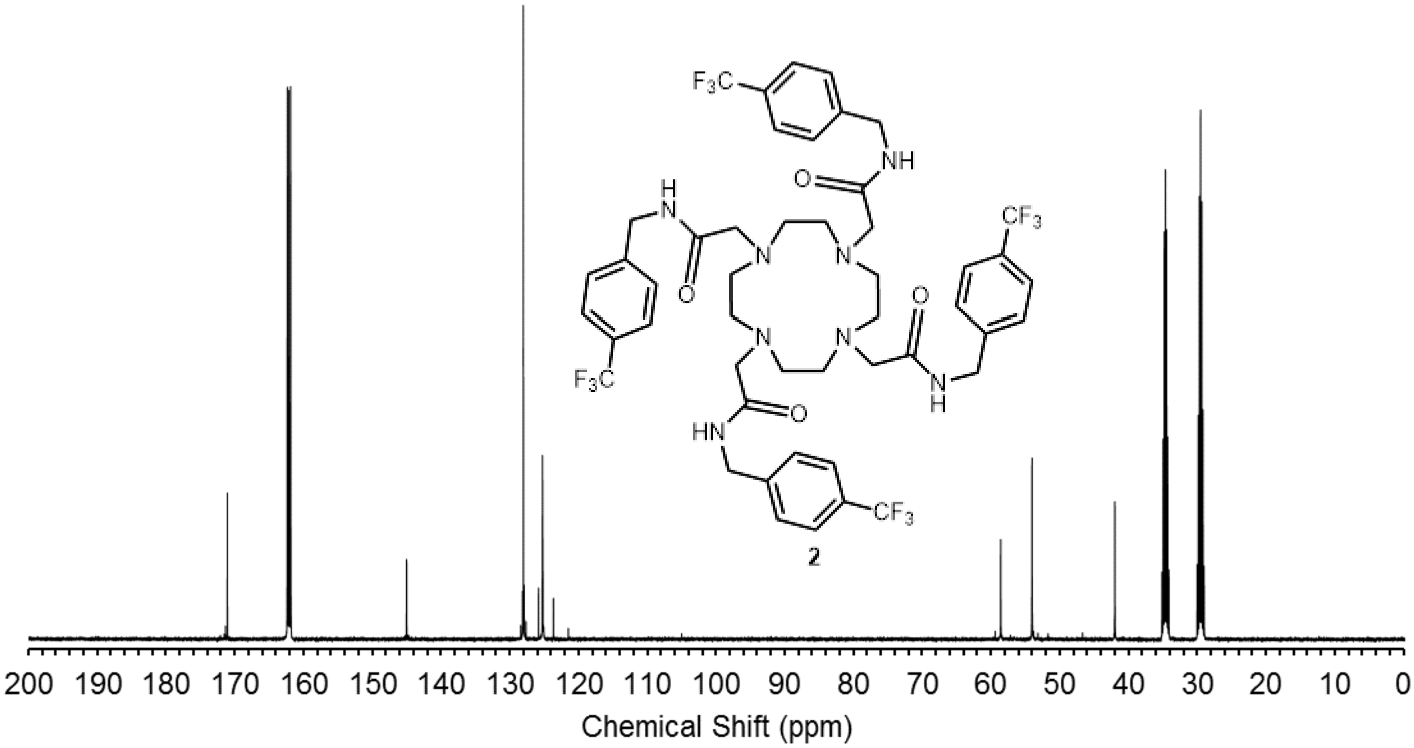

F$_3$C
NH
O
H
N
CF$_3$
N
N
O
O
N
N
F$_3$C
N
H
O
HN
CF$_3$
2
200 190 180 170 160 150 140 130 120 110 100 90 80 70 60 50 40 30 20 10 0
Chemical Shift (ppm)

^{19}F

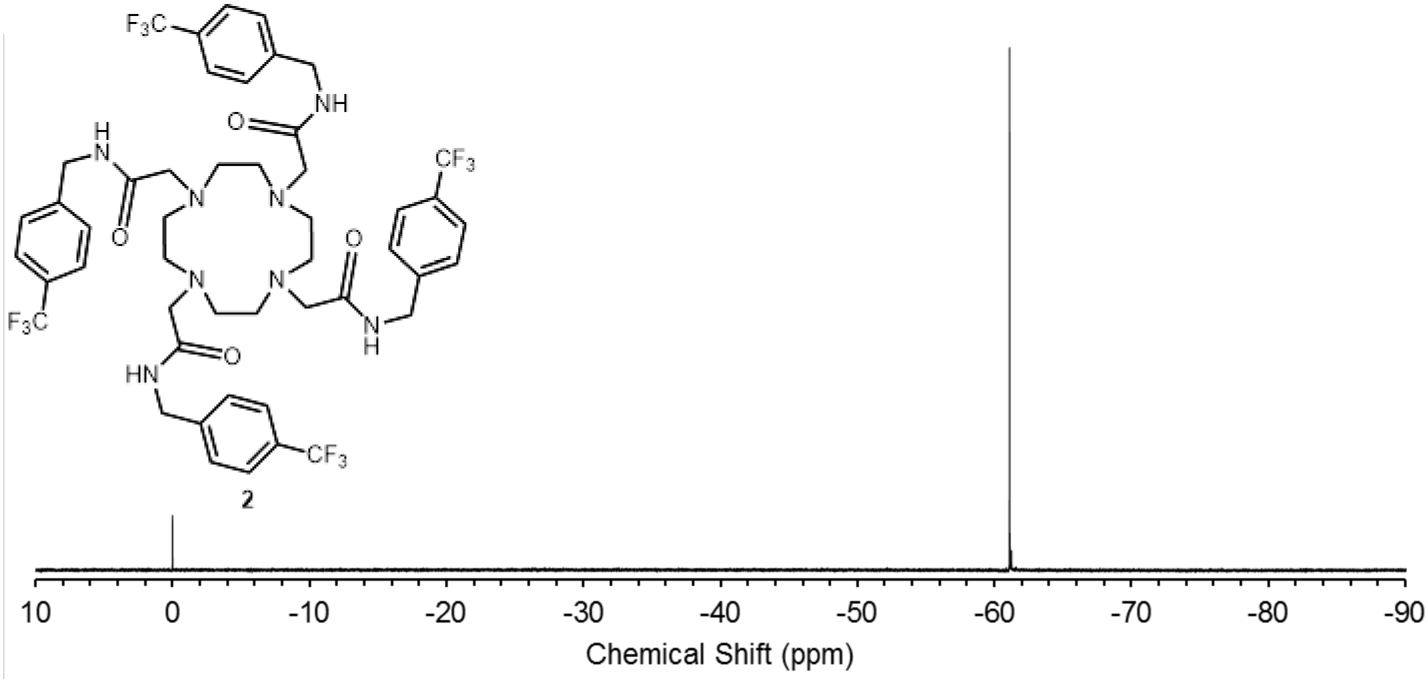

F$_3$C
NH
O
H
N
CF$_3$
N
N
O
O
N
N
F$_3$C
N
H
O
HN
CF$_3$
2
10 0 -10 -20 -30 -40 -50 -60 -70 -80 -90
Chemical Shift (ppm)

Europium(III) 2,2',2'',2'''-(1,4,7,10-tetraazacyclododecane-1,4,7,10-tetrayl)tetrakis-(*N*-(4-(trifluoromethyl)benzyl)acetamide) trichloride (2Eu^{III}): To a flask containing **2** (0.7916 g, 0.7619 mmol) and $EuCl_3·6H_2O$ (0.2601 g, 0.7106 mmol), CH_3OH (4 mL) and CH_3CN (20 mL) was added. The resulting mixture was heated at 60 °C. After 24 h, the mixture was filtered while hot through a fine glass frit, and the solvent was evaporated under reduced pressure. The crude product was crystallized from acetonitrile to yield a white solid (560 mg, 59%). ^{1}H NMR (400 MHz, D_2O): δ –13.14 (brs), –11.46 (brs), –8.17 (brs), –5.55 (brs), –2.86 (brs), 2.57 (brs), 3.11 (brs), 7.03 (brs), 7.09 (brs), 24.84 (brs); ^{19}F NMR (376 MHz, D_2O): δ –62.1 (s, C*F*$_3$); HRMS (*m*/*z*): $[M + 2Cl^-]^+$ calcd. for $C_{48}H_{52}F_{12}N_8O_4EuCl_2$, 1255.2509; found, 1255.2532 with expected isotope pattern; analysis (calcd., found for $C_{48}H_{52}F_{12}N_8O_4EuCl_3·6H_2O$): C (41.20, 41.65), H (4.61, 4.45), N (8.01, 8.45); Thermal gravimetric analysis (Supplementary Fig. S5) shows a mass loss of 7.7% corresponding to 6 H_2O, which is consistent with the combustion analysis.

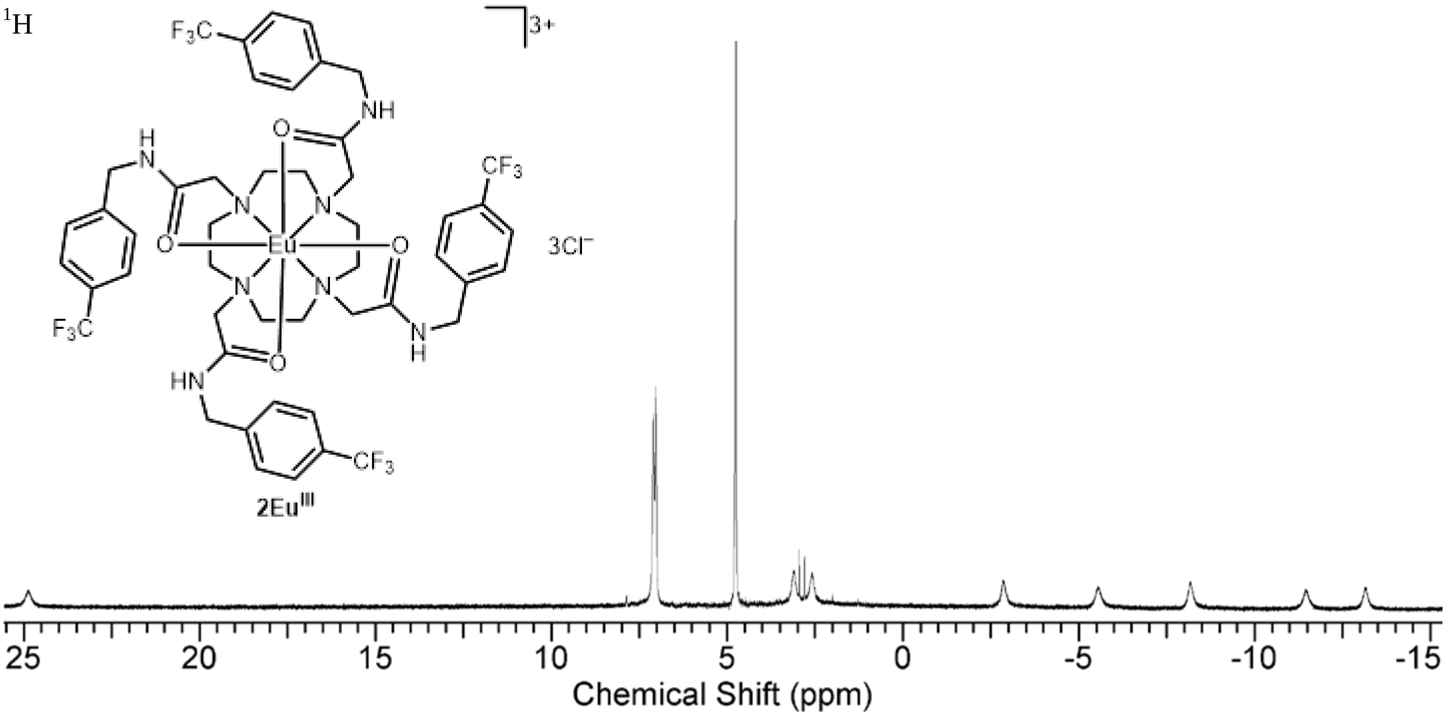

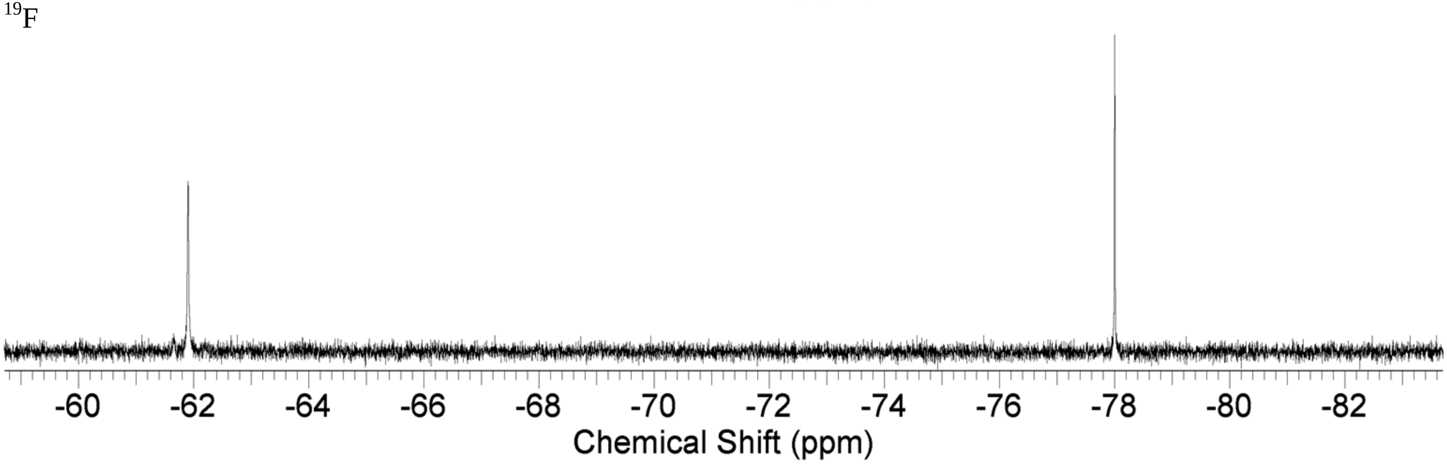

Europium(II) 2,2',2'',2'''-(1,4,7,10-tetraazacyclododecane-1,4,7,10-tetrayl)tetrakis-(*N*-(4-(trifluoromethyl)benzyl)acetamide) dichloride (2Eu^{II}): Under an atmosphere of N_2, a solution of **2Eu^{II}** (98 mg, 0.076 mmol) was dissolved in water (10 mL, degassed), and the pH of the resulting solution was adjusted to 6.5 using HCl (1 M, degassed, aqueous). To the resulting solution, Zn dust (150 mg, 2.3 mmol) was added, and the mixture was stirred vigorously for 30 minutes. The mixture was filtered through a 0.22 μm filter, and the filtrate was swirled with DOWEX-Na^+(0.1 g) for 1 minute and filtered with a 0.20 μm filter. The DOWEX step was repeated a total of three times to yield a pale-yellow solution of **2Eu^{II}** (quantitative). Solutions of **Eu^{II}1** were characterized with luminescence spectroscopy to confirm loss of Eu^{III} (Supplementary Figure S2),[1] and the concentration of **2Eu^{II}** was determined with EDXF spectroscopy.

2-Chloro-*N*-(4-methylbenzyl)acetamide (4): To a stirring solution of (4-(methyl)phenyl)methanamine (5.1969 g, 42.886 mmol) and triethylamine (4.80 mL, 34.4 mmol) in CH_2Cl_2 (5 mL) at 0 °C, a solution of chloroacetyl chloride (2.75 mL, 34.8 mmol) in CH_2Cl_2 (17 mL) was added dropwise. The resulting reaction mixture was stirred for 30 minutes at 0 °C followed by 30 minutes at ambient temperature. The mixture was filtered through a fine glass frit, and the solid was washed with CH_2Cl_2 (5 × 5 mL). The organic layer was washed with HCl (2 M, aqueous, 2 × 10 mL) followed by brine (3 × 10 mL), and the organic layer was dried over sodium sulfate. Solvent was removed under reduced pressure to yield an orange-brown solid that was crystallized from 1:1 petroleum ether/CH_2Cl_2 to yield a white solid (4.41 g, 52%) ^{1}H NMR (400 MHz, $CDCl_3$): δ 2.36 (s, 3H, C*H*$_3$), 4.07 (s, 2H, ClC*H*$_2$), 4.45 (d, ^1J = 5.4 Hz, 2H, C*H*$_2$N), 6.92 (brs, 1H, N*H*), 7.18 (dd, ^1J = 11.4, 8.6 Hz, 4H, C*H*); ^{13}C NMR (125 MHz, $CDCl_3$): δ 21.1 (*C*H$_3$), 42.6 (Cl*C*H$_2$), 43.6 (N*C*H$_2$), 127.8 (*C*H), 129.5 (*C*H), 134.3, 137.5, 165.7; HRMS (*m*/*z*): [M + Na]$^+$ calcd. for $C_{10}H_{12}ClNONa$, 220.0505; found, 220.0499.

^{1}H

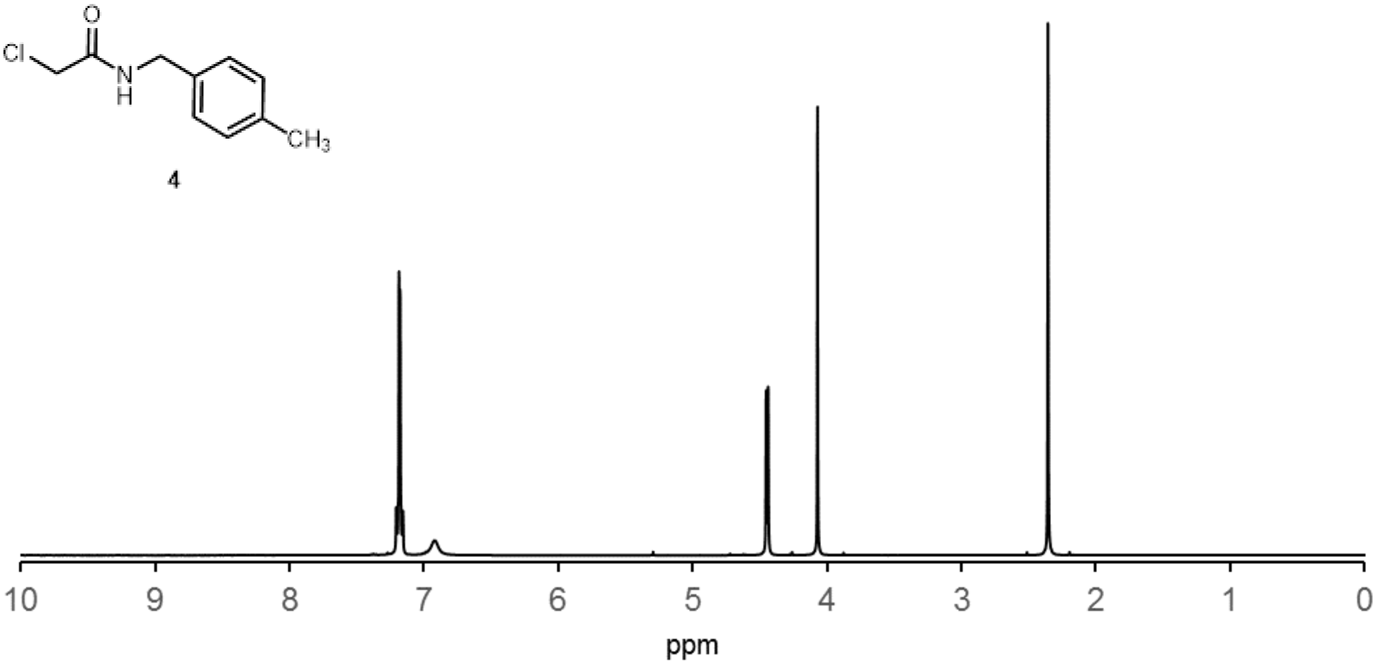

^{13}C

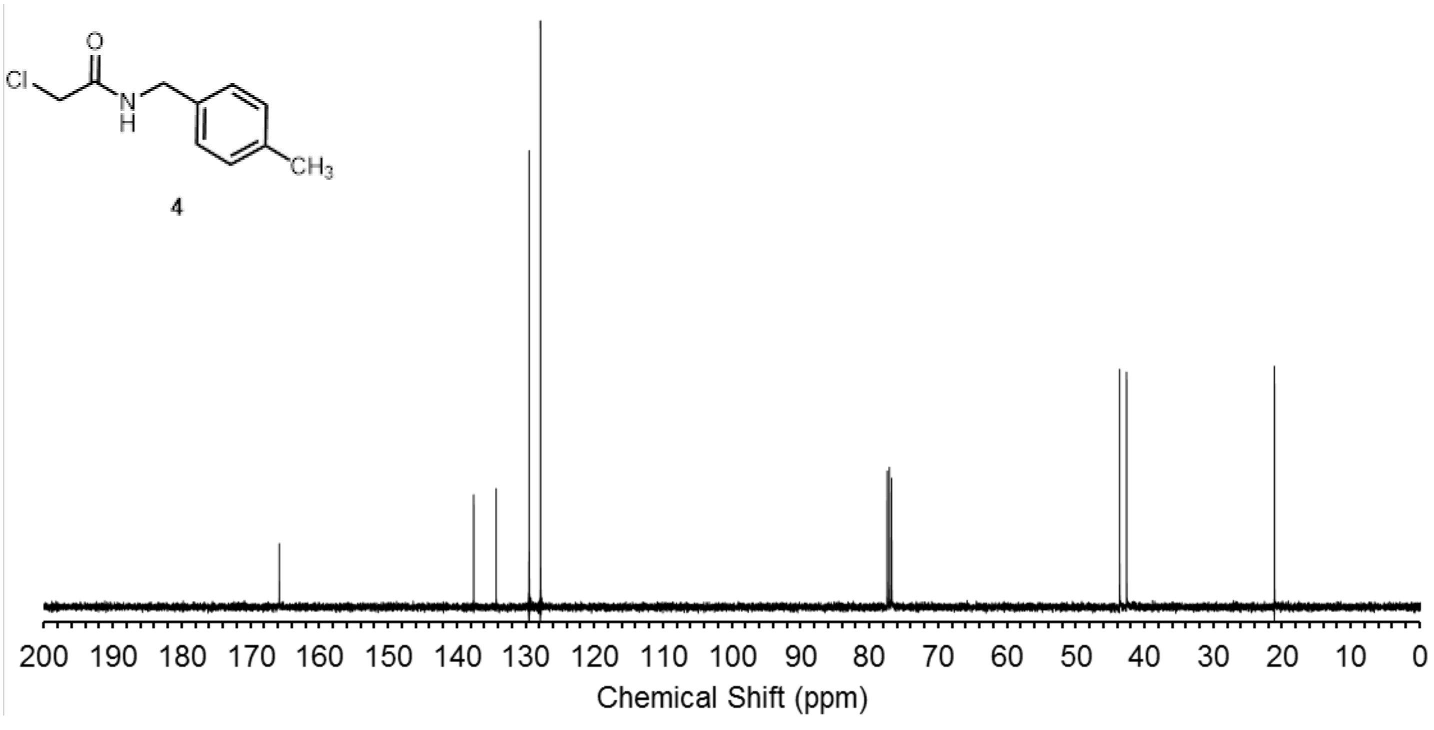

2,2',2'',2'''-(1,4,7,10-Tetraazacyclododecane-1,4,7,10-tetrayl)tetrakis-(*N*-(4-methylbenzyl)acetamide) (3): A stirring mixture of **4** (1.702 g, 8.607 mmol), Cs_2CO_3 (3.758 g, 19.48 mmol), cyclen (0.272 g, 1.58 mmol), potassium iodide (0.010 g, 0.060 mmol), and acetonitrile (50 mL) was heated to 120 °C. After 18 h, the mixture was filtered while hot through a fine glass frit, and the filtrate was concentrated under reduced pressure to yield a pale-yellow solid that was washed with water (50 mL) and ethanol (50 mL) to yield a white solid (878.8 mg, 58%). ^{1}H NMR (500 MHz, CH_3OD): δ 2.21 (s, 12H, CH_3), 3.41 (brs, ~16H*, CH_2CH_2), 3.81 (brs, 8H, CH_2), 4.22 (brs, 8H, CH_2), 7.02 (dd, *J* = 31.8, 7.4 Hz, 16H, C*H*), *peak overlaps with residual methanol peak, making exact integration impossible; ^{13}C NMR (125 MHz, DMSO-d_6): δ 20.6 (CH_3), 41.9 (CH_2), 49.7 (CH_2), 54.5 (CH_2), 127.2 (*C*H), 128.7 (*C*H), 135.6, 135.8, 167.1. HRMS (*m*/*z*): $[M + H]^+$ calcd. for $C_{48}H_{65}N_8O_4$, 817.5129; found, 817.5150.

^{1}H

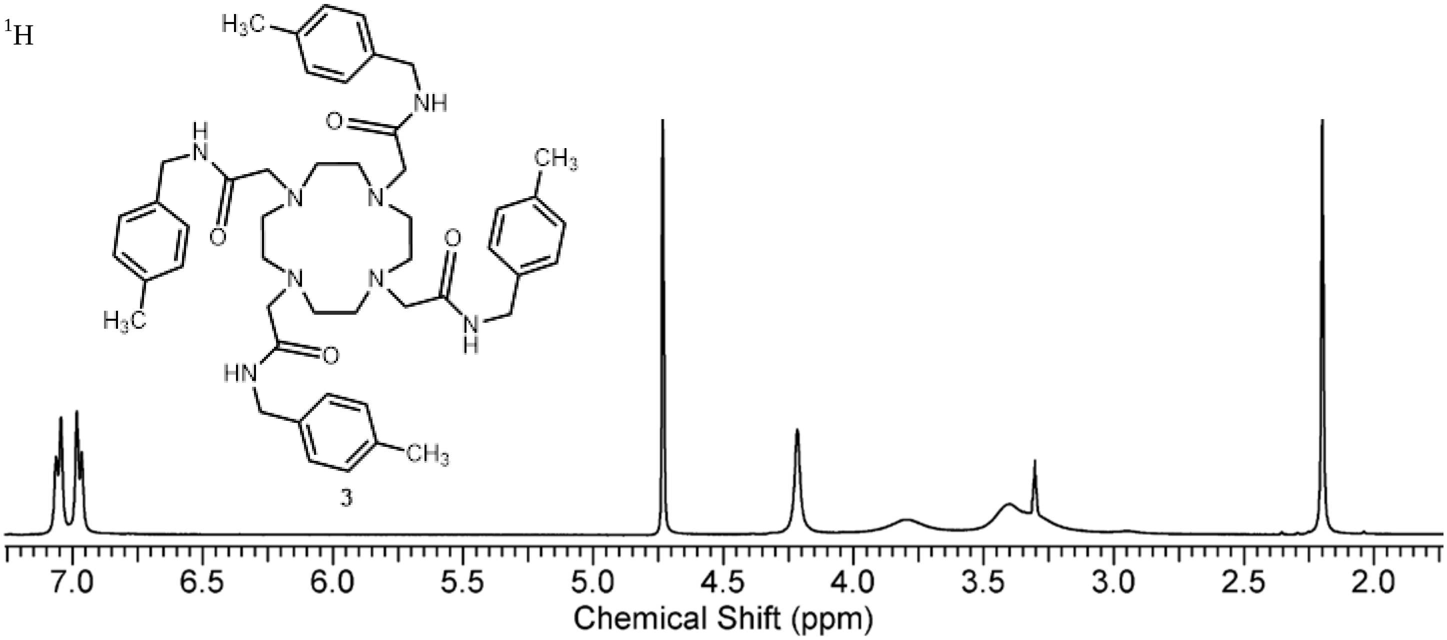

^{13}C

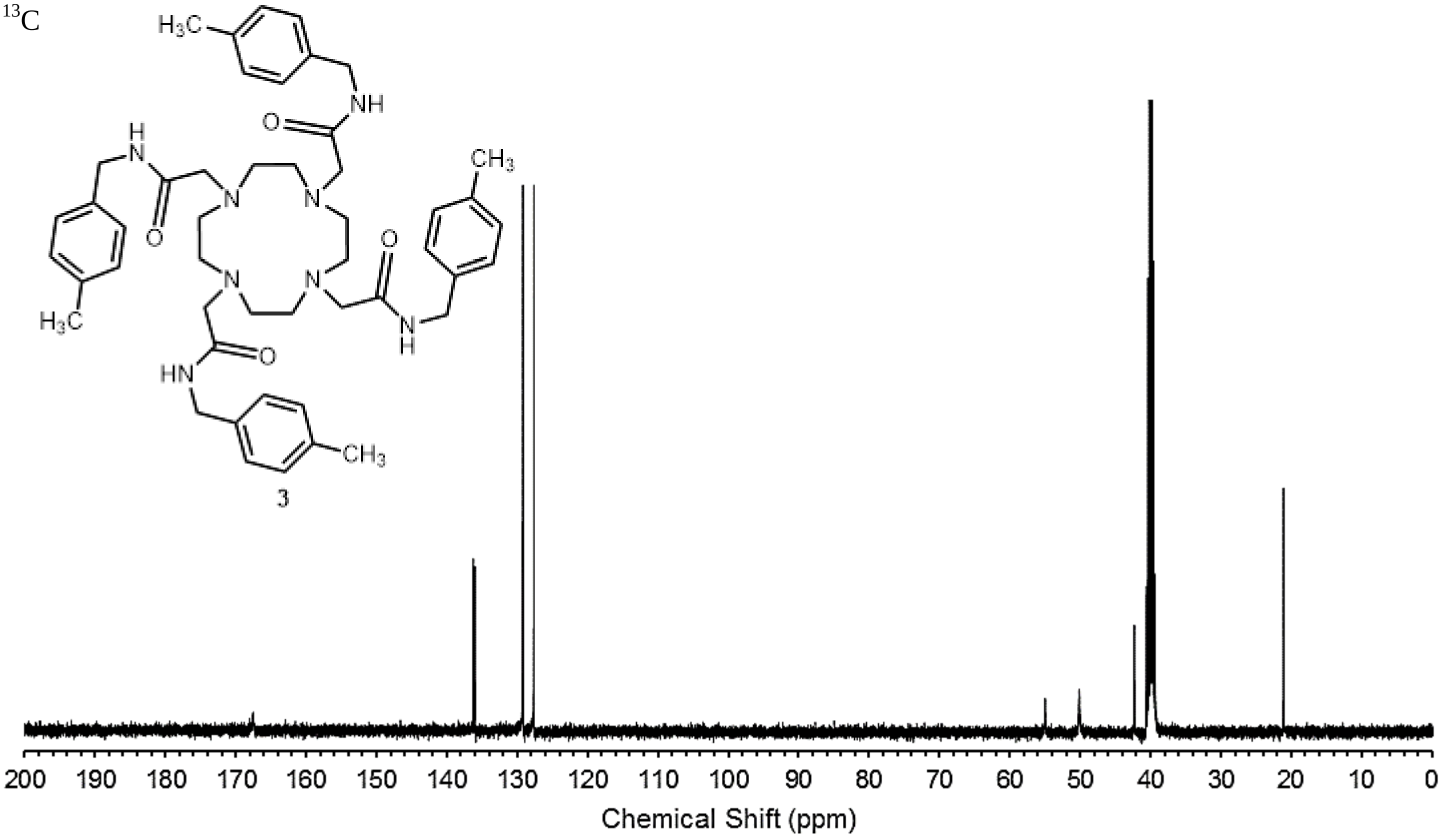

Europium(III) 2,2',2'',2'''-(1,4,7,10-tetraazacyclododecane-1,4,7,10-tetrayl)tetrakis(*N*-(4-methylbenzyl)acetamide) trichloride (3Eu^{III}): To a flask containing **3** (0.5404 g, mmol) and $EuCl_3$ (0.2382 g, mmol), CH_3OH (1 mL) and CH_3CN (50 mL) were added. The resulting mixture was heated at 60 °C. After 24 h, the mixture was filtered while hot through a fine glass frit, and the solvent was evaporated under reduced pressure. The crude product was dissolved in methanol (20 mL) and CH_2Cl_2 was added until a white precipitate formed. The precipitate was collected by filtration to yield a white solid (407 mg, 58%). ^{1}H NMR (400 MHz, D_2O): δ –13.89 (brs), –13.23 (brs), –7.80 (brs), –6.32 (brs), –2.52 (brs), 1.49 (brs), 2.25 (brs), 2.76 (brs), 6.25 (brs), 6.32 (brs), 26.91 (brs); HRMS (*m*/*z*): $[M + 2Cl^-]^+$ calcd. for $C_{48}H_{64}N_8O_4EuCl_2$, 1039.3640; found, 1039.3654; analysis (calcd., found for $C_{48}H_{64}N_8O_4EuCl_3{\cdot}6H_2O$): C (48.80, 48.74), H (6.31, 5.49), N (9.48, 10.02); Thermal gravimetric analysis (Supplementary Fig. S5) shows a 9.2% mass loss corresponding to 6 H_2O, which is consistent with the combustion analysis.

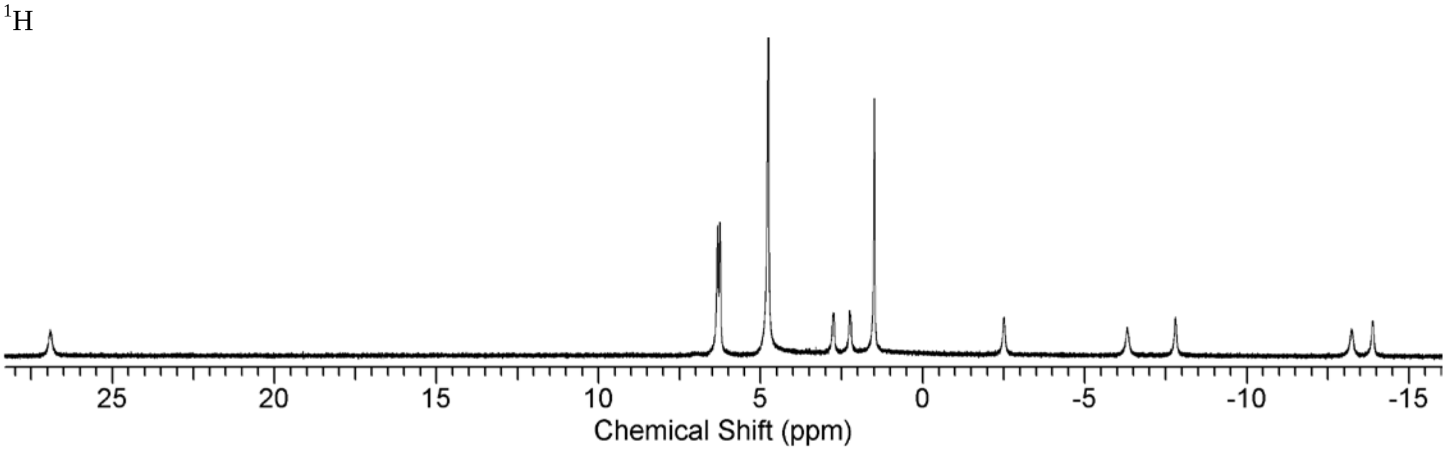

Europium(II) 2,2',2'',2'''-(1,4,7,10-tetraazacyclododecane-1,4,7,10-tetrayl)tetrakis(*N*-(4-methylbenzyl)acetamide) dichloride (3Eu^{II}): Under an atmosphere of N_2, a solution of **3Eu^{III}** (98 mg, 0.076 mmol) was dissolved in water (10 mL, degassed), and the pH of the resulting solution was adjusted to 6.5 using HCl (1 M, degassed, aqueous). To the resulting solution, Zn dust (150 mg, 2.3 mmol) was added, and the mixture was stirred vigorously for 30 minutes. The mixture was filtered through a 0.22 μm filter, and the filtrate was swirled with DOWEX-Na$^+$(0.1 g) for 1 minute and filtered with a 0.20 μm filter. The DOWEX step was repeated twice more to yield a pale-yellow solution of **3Eu^{II}** (quantitative). Solutions of **3Eu^{II}** were characterized with luminescence spectroscopy to confirm loss of Eu^{III} (Supplementary Figure S6).[1] The concentration of **3Eu^{II}** was determined with EDXF spectroscopy.

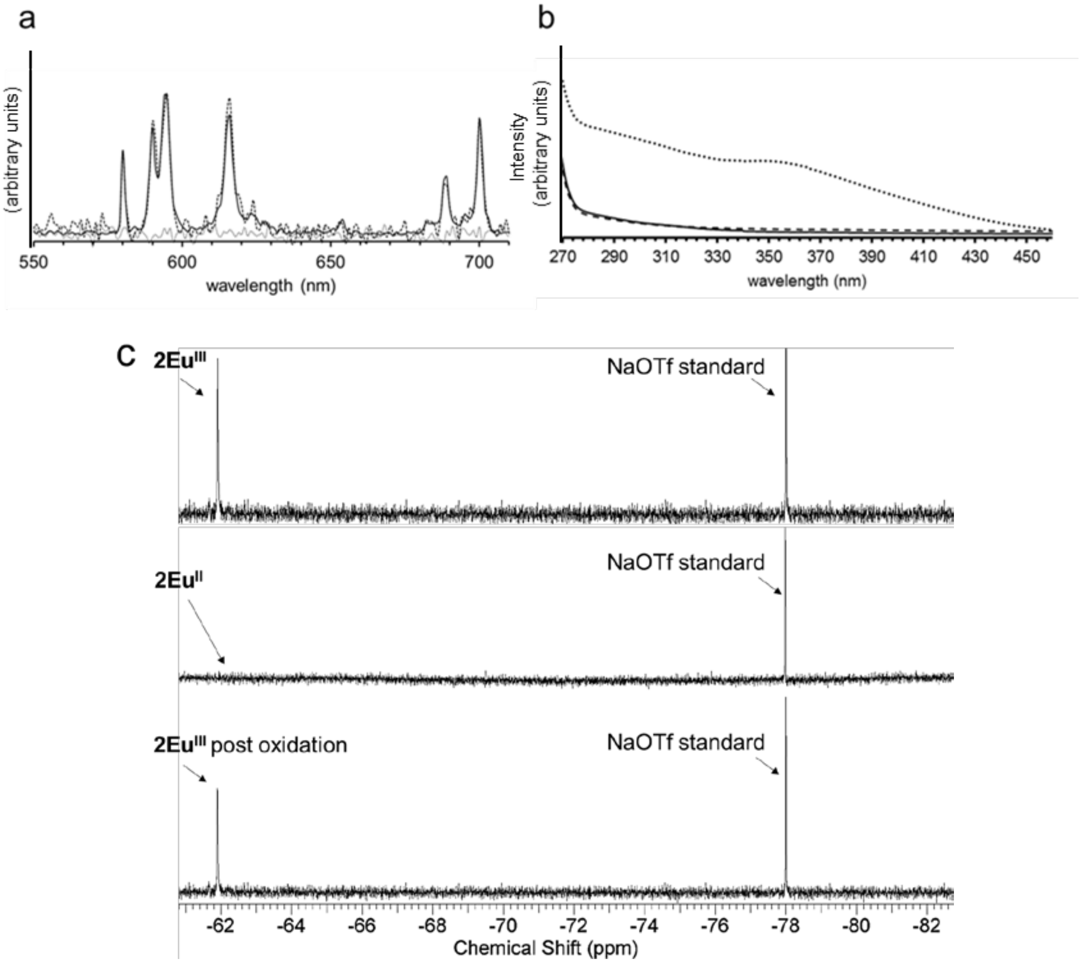

Figure S2. (a) Luminescence spectra of **2Eu**$^{\mathbf{III}}$ (–), **2Eu**$^{\mathbf{II}}$ (··), and **2Eu**$^{\mathbf{III}}$ post-oxidation (- -). Spectra were acquired in dimethylformamide (5 mM), λ_{ex} = 393 nm. After adding Zn^0, the Eu^{III} peaks disappear and upon allowing the yellow solution to oxidize, and the Eu^{III} peaks recover. The ratios of the peaks at 580 and 595 nm suggest that the Eu^{III} environment is similar for synthesized **2Eu**$^{\mathbf{III}}$ and oxidized **2Eu**$^{\mathbf{II}}$.[2] (b) Absorbance spectra of **2Eu**$^{\mathbf{III}}$ (–), **2Eu**$^{\mathbf{II}}$ (··), and **2Eu**$^{\mathbf{III}}$ post-oxidation (- -). Spectra were acquired in aqueous 3-(*N*-morpholino)propanesulfonic acid (1 mM, pH 7.0). (c) ^{19}F NMR spectra of **2Eu**$^{\mathbf{III}}$, **2Eu**$^{\mathbf{II}}$, and **2Eu**$^{\mathbf{III}}$ post-oxidation. Samples were 2–4 mM in aqueous 3-(*N*-morpholino)propanesulfonic acid (pH 7.0).

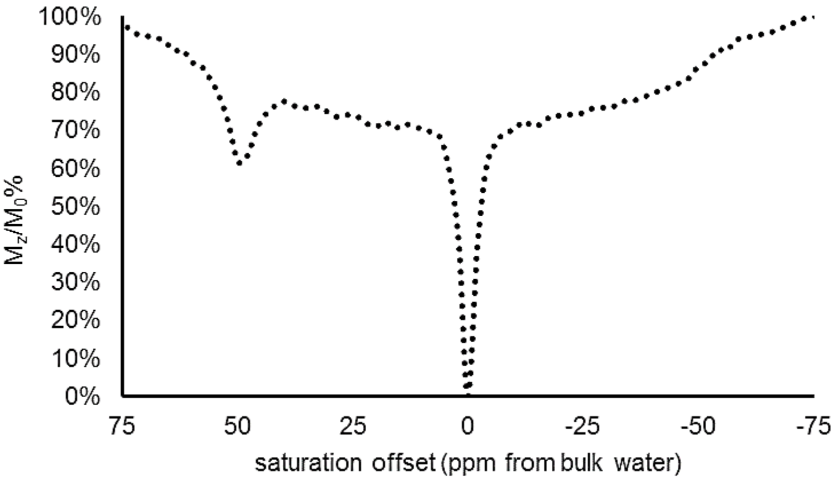

Figure S3. CEST spectrum of **2Eu**$^{\mathbf{II}}$ (pH 7.0) acquired at 11.7 T. **2Eu**$^{\mathbf{III}}$ has a saturation frequency offset of 49 ppm downfield from bulk water.

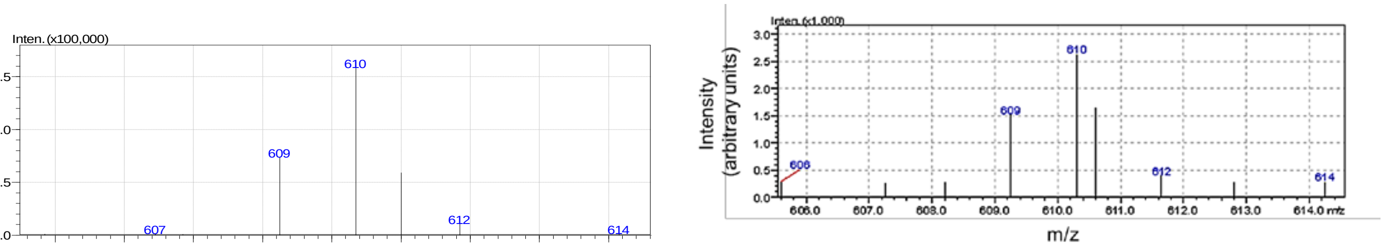

Figure S4. Mass spectra from LCMS of (left) $\mathbf{2Eu^{III}}$ and (right) mouse urine showing the mass-to-charge ratio for the ([M + Cl$^-$]$^{+2}$)/2 species of $\mathbf{2Eu^{III}}$ (1220/2 amu/charge = 610 *m*/*z*).

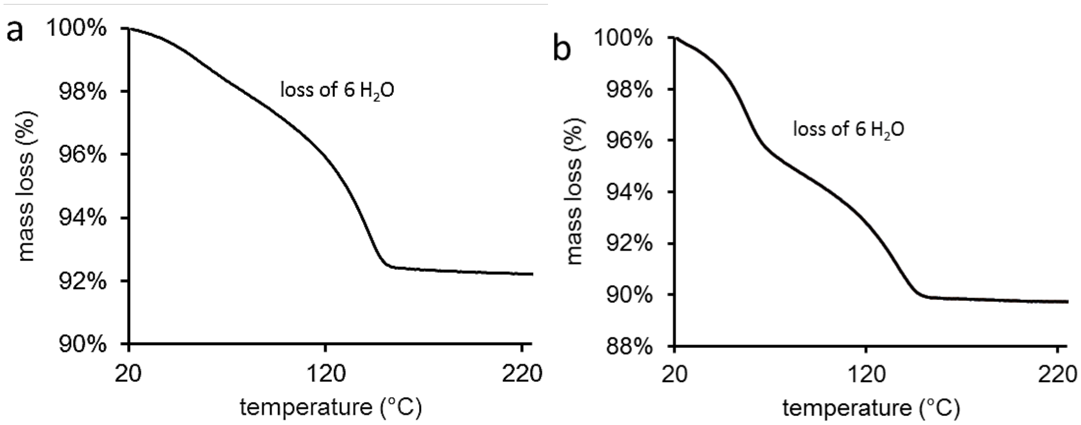

Figure S5. Thermogravimetric analyses of (a) $\mathbf{2Eu^{III}}$ and (b) $\mathbf{3Eu^{III}}$ recorded at 10 °C/min under flowing nitrogen.

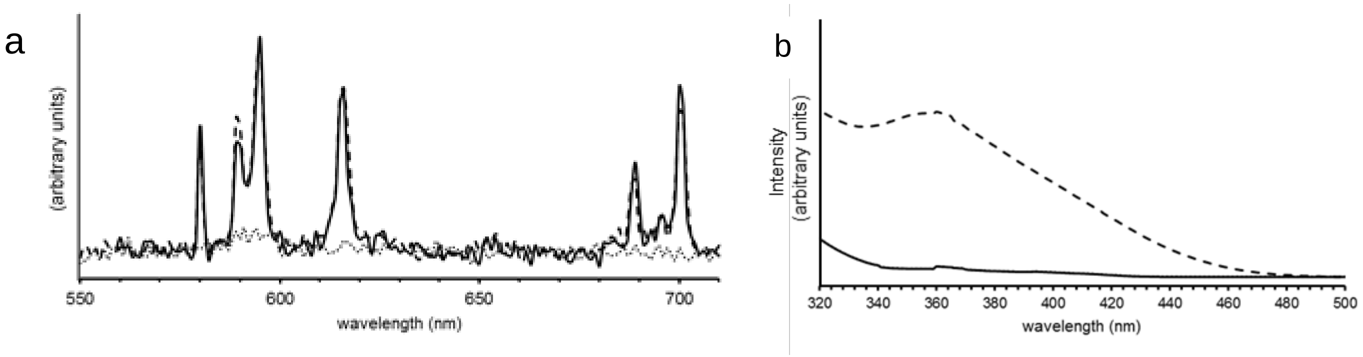

Figure S6. (a) Luminescence spectra of $\mathbf{3Eu^{III}}$ (–), $\mathbf{3Eu^{II}}$ (··), and $\mathbf{3Eu^{III}}$ post-oxidation (- -). Spectra were acquired in aqueous 3-(*N*-morpholino)propanesulfonic acid (pH 7.0, 5 mM) with λ_{ex} = 393 nm. After adding Zn^0, the Eu^{III} peaks disappear. Upon allowing the yellow solution to oxidize, the Eu^{III} peaks recover. The ratios of the peaks at 580 and 595 nm suggest that the Eu^{III} environment is similar for synthesized $\mathbf{3Eu^{III}}$ and oxidized $\mathbf{3Eu^{II}}$.[2] (b) Absorbance spectra of $\mathbf{3Eu^{III}}$ (–), $\mathbf{3Eu^{II}}$ (- -), and $\mathbf{3Eu^{III}}$ post-oxidation (··).

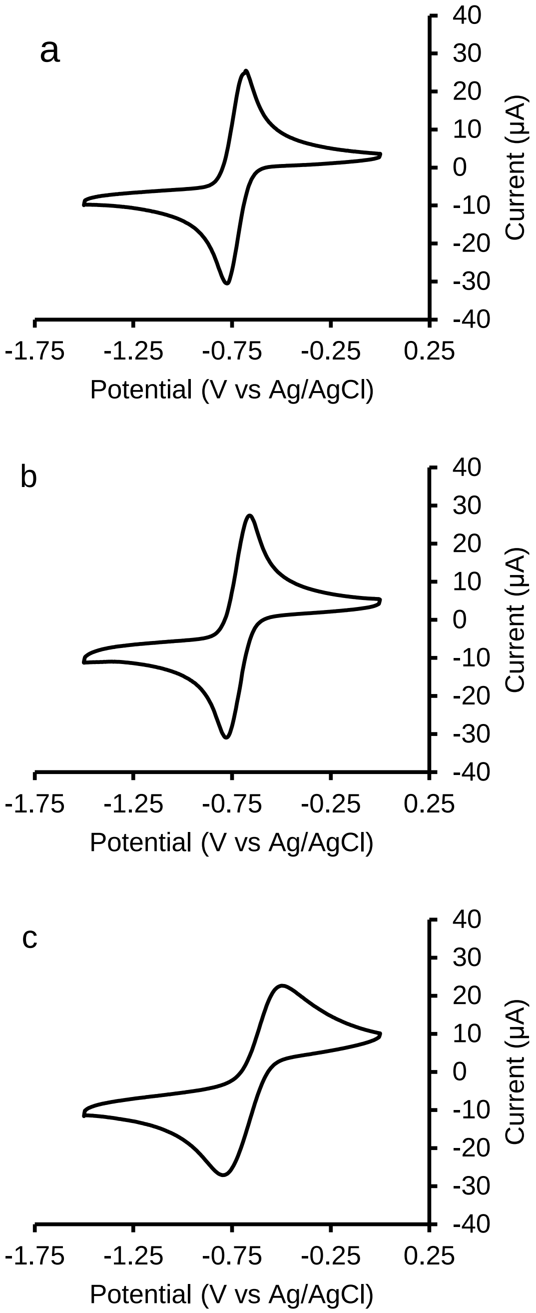

Figure S7. Representative cyclic voltammograms of solutions (3 mM in Eu) of (a) $\mathbf{2Eu}^{\mathrm{II/III}}$, (b) $\mathbf{3Eu}^{\mathrm{II/III}}$, and (c) $\mathrm{EuOTf_3}$ in dimethylformamide with tetraethylammonium perchlorate (150 mM) as the supporting electrolyte.

Table S1. Electrochemical data for **2Eu**, **3Eu**, and EuOTf$_3$.

$2Eu^{II/III}$

Trial	E_{ap} (V)	E_{cp} (V)	$E_{1/2}$ (V)
1	–0.675	–0.775	–0.725
2	–0.681	–0.775	–0.728
3	–0.681	–0.774	–0.728
Mean			–0.727
Standard deviation			0.002

$3Eu^{II/III}$

Trial	E_{ap} (V)	E_{cp} (V)	$E_{1/2}$ (V)
1	–0.660	–0.780	–0.720
2	–0.660	–0.780	–0.720
3	–0.660	–0.780	–0.720
Mean			–0.720
Standard deviation			0.0001

EuOTf$_3$

Trial	E_{ap} (V)	E_{cp} (V)	$E_{1/2}$ (V)
1	–0.499	–0.800	–0.649
2	–0.495	–0.794	–0.644
3	–0.499	–0.799	–0.649
Mean			–0.648
Standard deviation			0.003

Crystallographic Data

Data were collected on a Bruker Apex-II Kappa geometry diffractometer using Mo Kα radiation. The temperature of the crystals was maintained at 100 K using an Oxford Cryostream low-temperature device. Initial solutions were found using the method of intrinsic phasing via ShelXT[3] and further refined by the method of least squares using ShelXL[4] interfaced with both Olex2[5] and ShelXle.[6]

$2Eu^{III}$

A solution of **$2Eu^{III}$**Cl_3 (14 mg) in wet methanol (10 drops) was filtered through a 0.2 μm hydrophilic filter into a 5 mm NMR tube. After evaporation for three days, flake-like, clear, colorless crystals formed. The complex crystallized in space group *P*2/*n* with two disordered half molecules of **$2Eu^{III}$**Cl_3, one additional disordered *p*-CF_3 benzene unit, one inner-sphere water molecule, three outer-sphere chloride ions, and four outer-sphere water molecules in the asymmetric unit. The model was refined with a twin law (–1.0, 0.0, 0.0, 0.0, –1.0, 0.0, 1.0, 0.0, 1.0) with relatively low contribution (batch scale factors (BASF) = 0.0298(11)). All non-hydrogen atoms were refined anisotropically.

The CF_3 groups bound to carbons C38 and C14 were modeled to have two orientations for all fluorine atoms. Each CF_3 group was refined with a restrained carbon–fluorine distance (DFIX) of 1.328 Å with a standard deviation of 0.02 Å. Fluorine–fluorine distances inside of each CF_3 group were restrained with a fixed distance (DFIX) of 2.125 Å with a standard deviation of 0.02 Å. A rigid-body restraint (RIGU) was placed on each fluorine and the carbon of its CF_3 group with 1,2-distance standard deviation of 0.01 Å and a 1,3-distance standard deviation of 0.01 Å. Additional rigid-bond restraints (DELU) were placed between the carbons C23 and C47 and their fluorine atoms (F4, F5, and F6 with C23 and

F10, F11, and F12 with C47) with 1,2- and 1,3-distances of 0.01 Å. Fluorine atoms F8A, F12, F14A, F11, and F4 were refined with restrained atomic displacement parameters (ISOR) with a standard deviation of 0.02 Å.

Rigid-bond restraints (DELU) were placed between C12 and C13; C45 and C46; C34 and C41; C43 and C42; C29 and N1; and C29 and C30 with 1,2- and 1,3-distances of 0.01 Å. Carbon atoms C41, C42, C49, and C50 were refined with restrained atomic displacement parameters (ISOR) with a standard deviation of 0.001 Å. Carbon C31 was restrained to have similar atomic displacement parameters (SIMU) as N2 with a standard deviation of 0.04 Å. Carbon atom C11 was constrained to have the atomic displacement parameters (EADP) of C12. A benzene ring with its CF_3 carbon (C49, C50, C51, C52, C53, C54, and C55) and a benzene ring with its CF_3 carbon and benzylic methylene substituent (C34, C41, C42, C43, C44, C45, C46, and C48) were restrained to be flat (FLAT) with standard deviations of 0.1 Å.

Author response to PLAT220_ALERT_2_B: This alert concerns a possible erroneously assigned carbon atom in the ligand architecture based on the atomic displacement parameters. The ligand architecture is assigned based on NMR spectroscopy from other parts of the manuscript.

Author response to PLAT306_ALERT_2_B: This alert concerns an oxygen atom, O6, that has been refined without hydrogen atoms. This oxygen atom is part of a solvent molecule that is incorporated into the hydration layer. Acceptable hydrogen positions that do not crowd surrounding water molecules were not able to be found. As a consequence, the hydrogen atoms were removed.

Author response to PLAT417_ALERT_2_B: This alert concerns a relatively short contact of 1.94 Å between H7D and H9D, which are attached to water molecules in the hydration layer. A model in which no hydrogen crowing was present in this layer was not able to be obtained by the authors, and this relatively long crowding interaction was left as is.

Author response to PLAT420_ALERT_2_B: This alert concerns a water molecule (O3) without a hydrogen-bond acceptor. This is the water molecule bound to the europium ion, inside of the hydrophobic cage. For this reason, it is chemically unsurprising that there would be no hydrogen-bond acceptors.

Table S2. Crystallographic properties of $\mathbf{2Eu^{III}}Cl_3$:

Chemical Formula	$C_{48}H_{64}Cl_3EuF_{12}N_8O_{11}$
Formula Weight	1415.38
Temperature	100 K
Wavelength	0.71073 Å
Crystal System	Monoclinic
Space Group	*P*2/*n*
Unit Cell Dimensions	a = 10.8737(14) Å b = 26.268(4) Å c = 11.6670(14) Å $\alpha = 90^o$ $\beta = 117.775(7)^o$ $\gamma = 90^o$
Volume	2948.5(7) Å^3
Z	2
Density (calculated)	1.594 g cm^{-3}
Absorption Coefficient	1.300 mm^{-1}
F(000)	1436.0

$2Eu^{II}$

A solution of **$2Eu^{II}$**Cl_2 (15 mg) in ethanol (10 drops) in a wet glovebox (water allowed but no molecular oxygen) was filtered through a 0.22 μm hydrophilic filter into a 5 mm NMR tube. Dessication over three days led to yellow, block-like crystals. The complex **$2Eu^{II}$**Cl_2 crystallized in the space group *P*4/*n* with two quarters of **$2Eu^{II}$**, two outer-sphere chlorides, two inner-sphere water molecules, and two outer-sphere water molecules in the asymmetric unit. All non-hydrogen atoms were refined anisotropically. The asymmetric unit is split between two disordered parts. The majority of the atoms in PART 2 (C13, C14, N3, C15, C16, N4, C17, C18, C19, and C20) were refined with restrained atomic displacement parameters (ISOR) with a standard deviation of 0.06 Å.

Author response to PLAT215_ALERT_3_B: This alert concerns the min/max ADP ratios for C8 and C19, each having a ratio of 4.2 and each located in an aromatic ring. This alert suggests possible disorder. However, no disorder was able to modeled for these atoms.

Author response to PLAT220_ALERT_2_B, PLAT242_ALERT_2_B: These two alerts are due to the highly disordered nature of the second unit of **$2Eu^{II}$**Cl_2 in the asymmetric unit. The displacement parameters have made certain atoms appear to be assigned incorrectly. However, these atoms are all part of the ligand architecture used throughout the rest of the manuscript, and their identity is known based on NMR spectroscopy.

Author response to PLAT242_ALERT_2_B: This alert concerns the possibly miss-assignment of the Eu atom in the model. However, this material was shown through elemental analysis, X-ray fluorescence, and magnetic resonance experiments to contain europium. Therefore we are confident this is a complex of europium.

Author response to PLAT972_ALERT_2_B: This alert concerns calculated residual density near Eu1. This is an artifact of the Fourier cutoff and is commonly seen around heavy atoms.

Table S3. Crystallographic properties of **$2Eu^{II}$**Cl_2:

Chemical Formula	$C_{48}H_{46}Cl_2EuF_{12}N_8O_{6.66}$
Formula Weight	1292.43
Temperature	100 K
Wavelength	0.71073 Å
Crystal System	Tetragonal
Space Group	*P*4/*n*
Unit Cell Dimensions	a = 14.2597(12) Å b = 14.2597(12) Å c = 17.793(2) Å $\alpha = 90^o$ $\beta = 90^o$ $\gamma = 90^o$
Volume	3618.0(7) $Å^3$
Z	2
Density (calculated)	1.186 g cm^{-3}
Absorption Coefficient	1.013 mm^{-1}
F(000)	1297.0

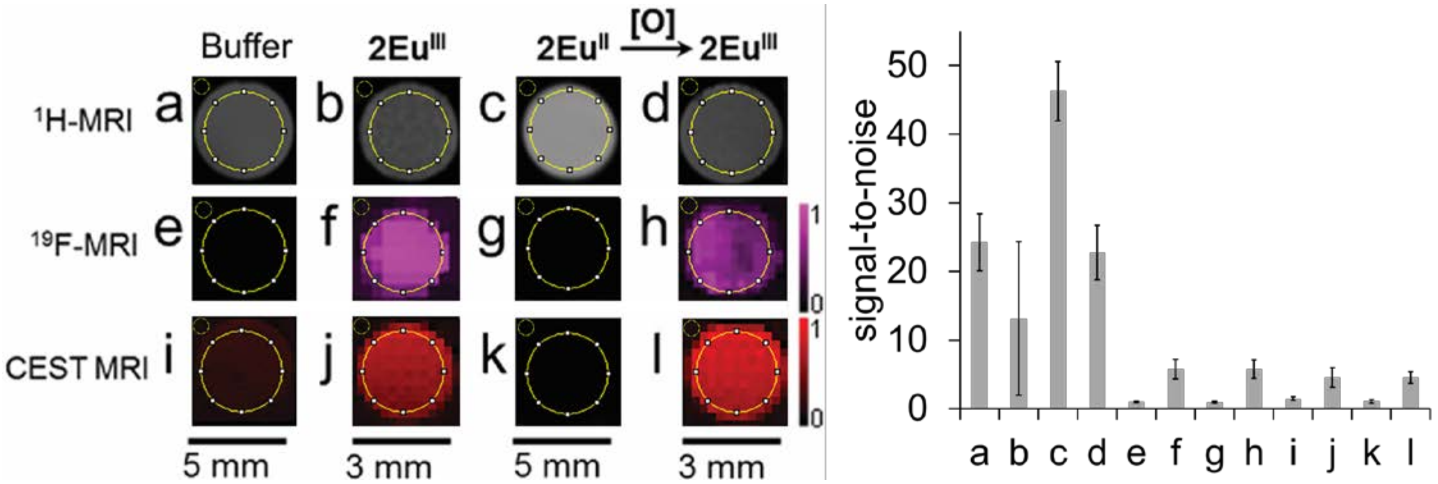

Figure S8. (left)The average pixel intensities within the larger yellow circles (signal) were divided by the average pixel intensities within the smaller yellow circles (background) to produce the signal-to-noise ratios in **Table S4**. (Right) Bar graph showing average signal-to-noise ratios. Error bars represent the standard deviations of the signal-to-noise ratios.

Table S4. Signal-to-noise (S/N) ratios for the images in **Figure S8** (**Figure 3** in the manuscript).

image	signal (S), arbitrary units with standard deviation in parentheses	noise (N), arbitrary units with standard deviation in parentheses	S/N with standard deviation in parentheses
a	73(2)	3(1)	24(4)
b	70(3)	5(4)	10(10)
c	143(2)	3.1(0.3)	46(4)
d	69(3)	3(1)	23(4)
e	3.1(0.2)	3.0(0.2)	1.0(0.1)
f	130(20)	22(5)	6(1)
g	3.1(0.2)	3.1(0.3)	1.0(0.1)
h	100(20)	17(3)	6(1)
i	25(2)	17(3)	1.5(0.3)
j	70(10)	15(4)	5(1)
k	3.9(0.4)	4(1)	1.1(0.2)
l	85(7)	19(3)	5(1)

References

1 L. A. Ekanger, D. R. Mills, M. M. Ali, L. A. Polin, Y. Shen, E. M. Haacke and M. J. Allen, *Inorg. Chem.*, 2016, **55**, 9981.
2 M. P. Bemquerer, C. Bloch, Jr., H. F. Brito, E. E. S. Teotino and M. T. M. Miranda, *J. Inorg. Biochem.*, 2002, **91**, 363.
3 G. M. Sheldrick, *Acta Cryst.*, 2015, **A71**, 3.
4 G. M. Sheldrick, *Acta Cryst.*, 2008, **A64**, 112.
5 O. V. Dolomanov, L. J. Bourhis, R. J. Gildea, J. A. K. Howard and H. Puschmann, *J. Appl. Cryst.*, 2009, **42**, 339.
6 C. B. Hübschle, G. M. Sheldrick and B. Dittrich, *J. Appl. Cryst.*, **44**, 2011, 1281.